

Article

Identification and Characterization of a Highly Active Hyaluronan Lyase from *Enterobacter asburiae*

Linjing Zhang¹, Jiayu Jiang¹, Wei Liu¹, Lianlong Wang¹, Zhiyuan Yao¹, Heng Li^{1,*}, Jinsong Gong¹, Chuanli Kang², Lei Liu², Zhenghong Xu³ and Jinsong Shi^{1,*}

¹ Key Laboratory of Carbohydrate Chemistry and Biotechnology, Ministry of Education, School of Life Sciences and Health Engineering, Jiangnan University, Wuxi 214122, China

² Shandong Engineering Laboratory of Sodium Hyaluronate and Its Derivatives, Shandong Focusfreda Biotech Co., Ltd., Qufu 273165, China

³ Innovation Center for Advanced Brewing Science and Technology, College of Biomass Science and Engineering, Sichuan University, Chengdu 610065, China

* Correspondence: liheng@jiangnan.edu.cn (H.L.); shijs@163.com (J.S.)

Abstract: Hyaluronic acid (HA) is a well-known functional marine polysaccharide. The utilization and derivative development of HA are of great interest. Hyaluronan lyase has wide application prospects in the production of HA oligosaccharides and lower molecular weight HA. In this study, a strain of *Enterobacter asburiae* CGJ001 with high hyaluronan lyase activity was screened from industrial wastewater. This strain exhibited an impressive enzyme activity of 40,576 U/mL after being incubated for 14 h. Whole genome sequencing analysis revealed that *E. asburiae* CGJ001 contained a cluster of genes involved in HA degradation, transport, and metabolism. A newly identified enzyme responsible for glycosaminoglycan degradation was designated as HylEP0006. A strain of *E. coli* BL21(DE3)/pET-22b(+)-hylEP0006 was successfully constructed. HylEP0006 exhibited optimal degradation at 40 °C and pH 7.0, showing a high activity of 9.5×10^5 U/mg. HylEP0006 showed specific activity against HA. The minimum degradation fragment of HylEP0006 was hyaluronan tetrasaccharides, and HylEP0006 could efficiently degrade HA into unsaturated disaccharides (HA₂), with HA₂ as the final product. These characteristics indicate that HylEP0006 has a potential application prospect for the extraction and utilization of hyaluronic acid.

Keywords: hyaluronan lyase; hyaluronic acid; hyaluronic acid oligosaccharides; *Enterobacter asburiae*



Citation: Zhang, L.; Jiang, J.; Liu, W.; Wang, L.; Yao, Z.; Li, H.; Gong, J.; Kang, C.; Liu, L.; Xu, Z.; et al. Identification and Characterization of a Highly Active Hyaluronan Lyase from *Enterobacter asburiae*. *Mar. Drugs* **2024**, *22*, 399. <https://doi.org/10.3390/md22090399>

Academic Editor: Azizur Rahman

Received: 31 July 2024

Revised: 24 August 2024

Accepted: 28 August 2024

Published: 31 August 2024



Copyright: © 2024 by the authors. Licensee MDPI, Basel, Switzerland. This article is an open access article distributed under the terms and conditions of the Creative Commons Attribution (CC BY) license (<https://creativecommons.org/licenses/by/4.0/>).

1. Introduction

Hyaluronic acid (HA) is a sticky high-molecular-weight polysaccharide, with the unbranched disaccharide of *N*-acetyl glucose and *D*-glucuronic acid linked through β -1,4 glycoside bond as repeating units connected through β -1,3 glycosidic bonds [1]. The unique properties of HA, including high viscoelasticity and plasticity, exceptional water retention capacity, and permeability, have led to it being extensively utilized in the fields of medicine, clinical diagnosis, cosmetics, and health food industries [2].

Traditionally, hyaluronic acid is mainly obtained from mammalian tissues, including the rooster comb, cartilage, and umbilical cord. Despite the high cost of production, the process is relatively complex, and the large-scale preparation is difficult. The exploration of glycoconjugates originating from microorganisms, especially marine organisms, is gaining increasing attention due to the concern generated by bovine spongiform encephalopathy (BSE) and other food chain crises. Current research focuses on the utilization of inherently secure aquatic organisms as raw materials, aiming to not only promote waste utilization and comprehensive development but also reduce the extraction cost of hyaluronic acid [3]. The rational utilization of marine hyaluronic acid resources can play a comprehensive role in the development and waste utilization effect.

Recent studies have shown that the biological activities of HA are directly related to their relative molecular weight (Mw). In contrast, HA with different molecular weights can exhibit opposite biological activities [4,5]. The HA polymer with higher molecular weight ($M_w > 2 \times 10^6$ Da) has outstanding properties of elasticity and moisturizing and the function of inflammation inhibition and lubrication, which is commonly used for ophthalmic surgery adhesives and joint injection in ophthalmic surgery [6]. The HA with Mw of $(1-2) \times 10^6$ Da exerts preferable lubrication, moisturizing, and drug slow-release properties, which can be applied in cosmetics, eye drops, skin burn healing, and postoperative anti-adhesion [7]. The HA with lower molecular weight ($M_w \leq 1 \times 10^4$ Da) (including Hyaluronan oligosaccharides, o-HAs) has demonstrated immunological activities of activating endothelial cells and inhibiting multidrug resistance in tumors [8,9], which could be broadly applied in medicine. Comparatively, HA with lower molecular weight can maintain its activities while being readily absorbed by the human body [10]. Consequently, research on HA with lower molecular weight has been a focal point [11].

At present, HA with lower molecular weight is mainly obtained through the degradation of HA with high molecular weight by physical (ultrasonication, microwave irradiation, and heating), chemical (acidic and alkaline hydrolysis, oxidant hydrolysis), and enzymatic methods. The resultant products employing either physical or chemical methodologies usually comprise a composite of polydisperse oligosaccharides and monosaccharides [12], complicating subsequent purification processes and making it challenging to obtain HA oligosaccharides with particular molecular weight. Moreover, HA oligosaccharides can also be synthesized from its monosaccharide precursor through chemical methods. However, time-consuming reaction processes, rare carbohydrate oligosaccharide backbones, and expensive substrates (uridine diphosphate (UDP)-sugars) obstruct the large-scale production of HA oligosaccharides [13]. In contrast, the utilization of well-characterized hyaluronidase (HAase) enzymes for producing HA oligosaccharides presents a highly promising and appealing alternative, owing to its distinctive advantages of mild operating conditions, high degradation rates, and high product homogeneity [14]. Microbial-derived hyaluronidase is plentiful, easy to recombinant expression, convenient for extraction, and relatively simple for high purification. Therefore, it is the primary source of enzyme for application. Since the significance of bacterial hyaluronidase, various microorganisms have been explored to produce hyaluronidase. Recently, it was reported that *Bacillus* sp. A50 produced hyaluronic acid lyase from the deep sea [15], and a hyaluronic acid lyase (BniHL) was purified from *Bacillus niacin* strain JAM F8 [16]. A hyaluronate lyase was found in *Haliscomenobacter hydrossis* from active sludge, which was rich in the microorganism community, playing an important role in treating public wastewater [17]. However, current progress in lower enzyme activity, unclear degradation products, and low yield limit the production of hyaluronidase and industrial production of oligosaccharides by enzymatic methods. Consequently, it is necessary to obtain better microbial hyaluronidase and clarify the characteristics for HA industry promotion.

Therefore, this study aims to screen and isolate microorganism strains harboring high-activity hyaluronan lyase and characterize the enzymatic properties of the obtained hyaluronan lyase to supplement the enzyme resources further.

2. Results

2.1. Isolation and Identification of *Enterobacter* sp. CGJ001

The strain *Enterobacter* sp. CGJ001 was successfully screened from industrial wastewater, which can grow well in culture with the single carbon source of hyaluronic acid. The strain of *Enterobacter* sp. CGJ001 was cultured by fermentation and reached a stable growth phase at 12 h. A large amount of hyaluronic acid lyase (intracellular enzyme activity) began to be produced around 6 h and reached the highest level of enzyme activity, 40,576 U/mL at 14 h, as shown in Figure 1.

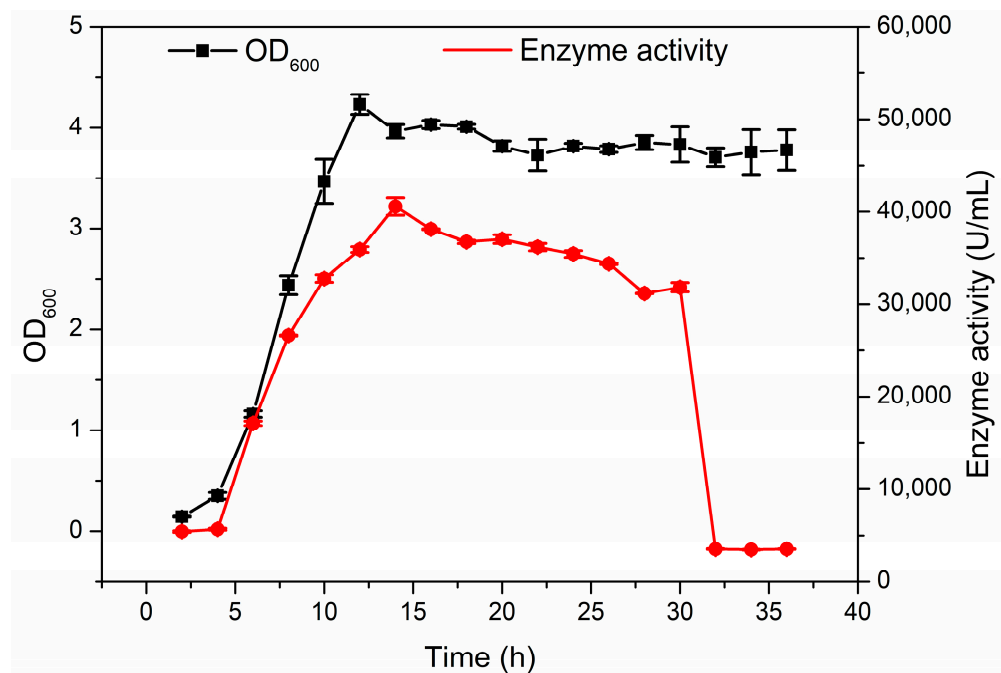


Figure 1. Typical time course of the growth of *Enterobacter* sp. CGJ001 in a shake flask. Enzyme activity (red, U/mL) and cell growth density (black, OD₆₀₀ values) were measured regularly. Values represent the mean of three replicates \pm SD.

The length of the 16S rDNA sequence from strain *Enterobacter* sp. CGJ001 was found to be 1381 bp. A sequence blast alignment was conducted using the NCBI database to investigate its phylogenetic relationship, and a set of 14 type strains were chosen for further analysis. The phylogenetic tree analysis revealed that strain *Enterobacter* sp. CGJ001 exhibited the highest similarity of 99.85% with *Enterobacter asburiae* JCM6051 (NR 024640.1), as depicted in Figure 2. Consequently, strain *Enterobacter* sp. CGJ001 was designated as *Enterobacter asburiae* CGJ001.

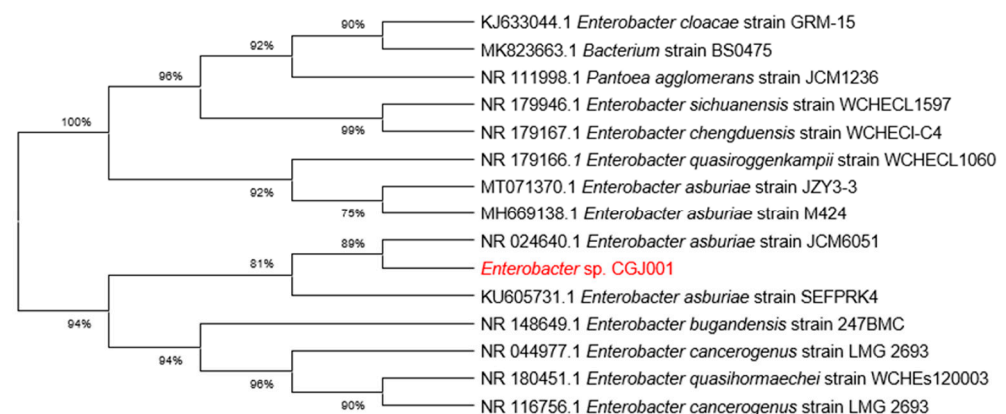


Figure 2. The phylogenetic tree of strain *Enterobacter* sp. CGJ001 was constructed based on the analysis of 16S rDNA sequences, and the phylogenetic tree was generated by MEGA X using the neighbor-joining method.

2.2. Whole-Genome Analysis of *E. asburiae* CGJ001 and Prediction of PUL_{HA}

Whole-genome sequencing analysis showed that the complete genome of *E. asburiae* CGJ001 was composed of the main chromosome of 4,610,415 bp and one plasmid, which was named plasmid A (265,602 bp), with an overall GC content of 57.18%. Its chromosomes contained 4425 total genes, 82 tRNAs, 25 rRNAs, and 200 tandem repeats, as shown in

Figure 3a and Table 1. The 4193 coding genes in the whole genome of *E. asburiae* CGJ001 were compared with the database to obtain the functional KEGG, GO, and COG annotation information. A total of 2991 genes were functionally annotated in the KEGG database, as shown in Figure 3b, of which 1667 genes were annotated in various metabolic pathways, and mainly distributed in metabolic pathways and environmental information processing pathways. The most number of genes in the metabolic pathway was located in carbohydrate metabolism (472 genes). The annotation of 472 genes indicated *E. asburiae* CGJ001 had intense functions of carbohydrate catabolism and metabolism. As shown in Figure 3c, COG database annotation results showed that functional proteins related to the transport and metabolism of carbohydrate substances and amino acids were highly annotated, indicating that this strain had a strong ability for carbohydrate metabolism. In addition, Figure 3d showed that 3629 genes could be annotated in GO database with three kinds of function. Among the molecular functions, the top annotated function in the number of genes was catalysis (792), followed by binding and transport. Genes annotated to the biological process also count high, with metabolic and cellular process as the two main classifications. Those genes related to cell components were mainly annotated in cells, cell components, and organelles.

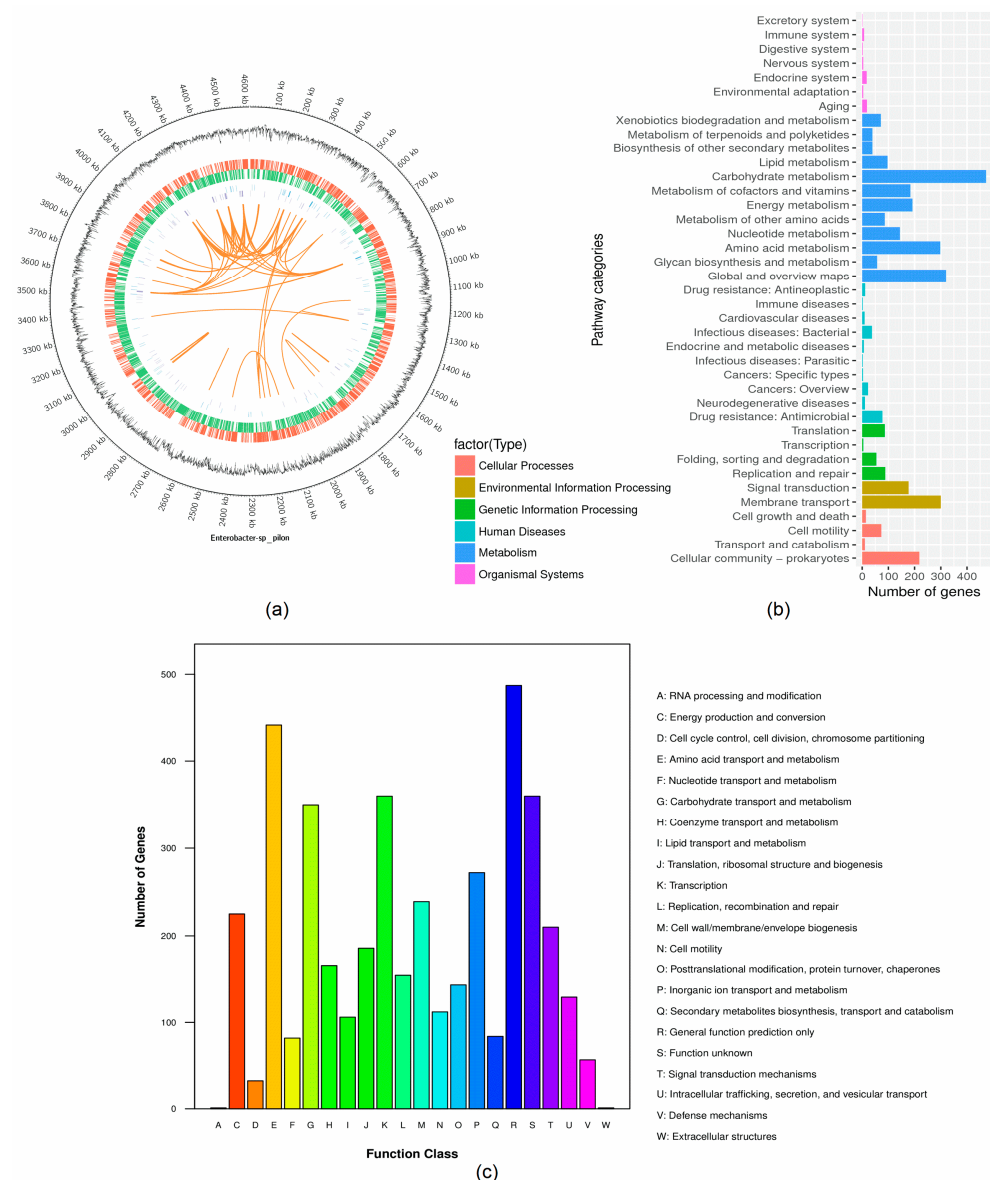


Figure 3. Cont.

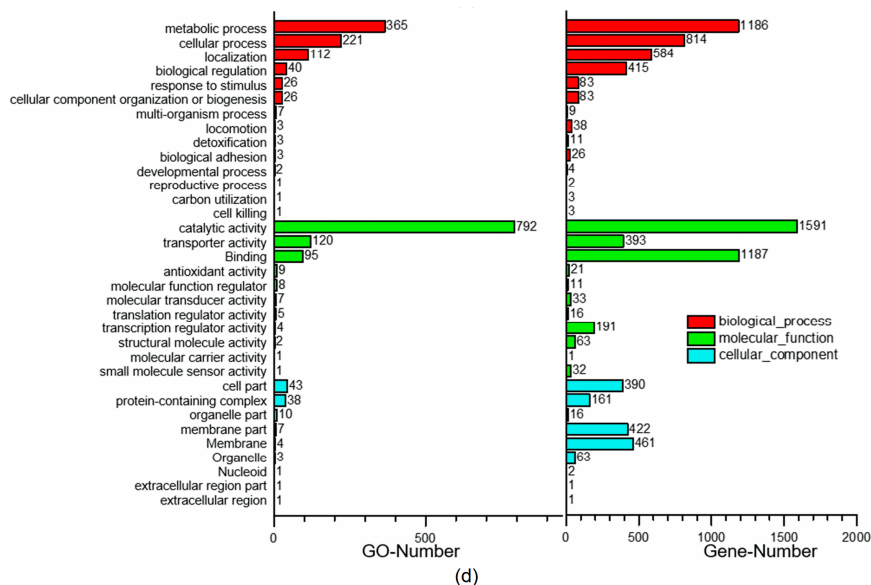


Figure 3. Whole-genome analysis of *E. asburiae* CGJ001: (a) Chromosome genome pattern of *E. asburiae* CGJ001. The circle diagram shows seven kinds of information, from outside to inside: The first circle is the genomic position information, the second circle is the GC content information, the third circle is the coding genes on the plus strand (red marks), the fourth circle is the coding genes on the minus strand (green marks), the fifth circle is the ncRNA information on the plus strand (blue marks), and the sixth circle is the ncRNA information on the minus strand (purple marks). The seventh circle is marked with information on long genomic repeats (orange marks). (b) KEGG metabolic pathway secondary classification of *E. asburiae* CGJ001. KEGG classified the biological metabolic pathways into 6 categories, and each category was systematically divided into secondary classifications. The number of genes in each metabolic pathway in the secondary classification was counted. (c) COG functional classification statistics of *E. asburiae* CGJ001. (d) GO functional classification statistics of *E. asburiae* CGJ001.

Table 1. *E. asburiae* CGJ001 genome basic information.

Feature	Chromosome	Plasmid A
Size (bp)	4,610,415	265,602
G + C content (%)	55.91	48.33
Total genes	4425	505
Protein-coding genes	4193	505
rRNA	25	0
tRNA	82	0
Repeat genes	200	0

2.3. Prediction of PUL_{HA}

The genes associated with HA utilization in strain *E. asburiae* CGJ001 clustered in a genomic region of plasmid A, as shown in Figure 4a, suggesting that this gene cluster might be the polysaccharide utilization site of HA (PUL_{HA}). The PUL_{HA} in the genome consisted of six components: PL8 family hyaluronan lyase (EP0006), two GH88 family unsaturated glucuronate hydrolases, and a sugar transporter glucose phosphotransferase system (PTS) (Figure 4b). Since this enzyme is an intracellular enzyme, it is hypothesized that hyaluronan lyase PL18 is embedded on the cell surface and degrades hyaluronan to unsaturated disaccharides. Unsaturated disaccharides are transported to the cytoplasmic periphery by the TonB transport system and then imported into the cytoplasm by the sugar transporter glucose phosphorylase system PTS. The degradation process facilitated by the unsaturated glucuronate hydrolase GH88 undergoes within the cytoplasm, forming 4,5 unsaturated glucuronic acid (Δ GlcUA) and *N*-acetyl D-glucosamine (GlcNAc) through

the cleavage of β -1,4 bonds. Δ GlcUA and GlcNAc are subsequently involved in further metabolism processes.

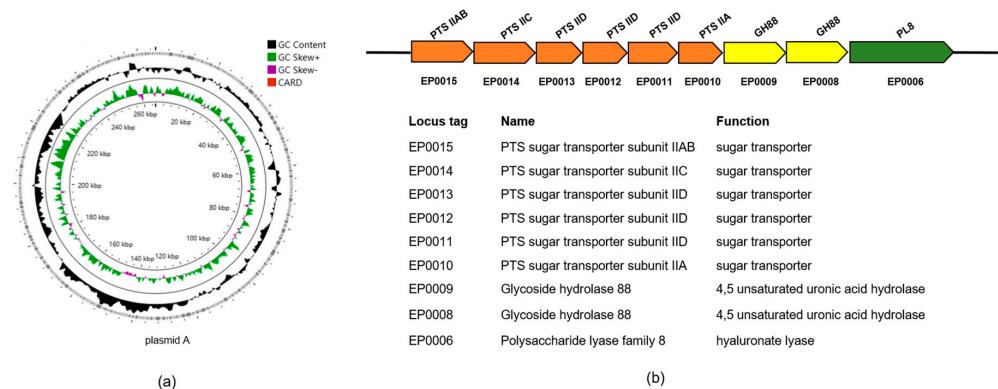


Figure 4. The analysis of plasmid A: (a) Plasmid A genome pattern of *E. asburiae* CGJ001. (b) The PUL_{HA} was anticipated in plasmid A of strain *E. asburiae* CGJ001.

The Hyaluronan Lyase (*hyleP0006*) gene has a length of 2397 bp and encodes a protein consisting of 799 amino acid residues. The predicted Mw and isoelectric point (pI) values of HyleP0006 are 87.93 kDa and 8.68, respectively. By utilizing SignalP-5.0, we identified a type I signal peptide at the N-terminus of HyleP0006 composed of 20 amino acid residues (MKKTNLAFSLLCLSMGSVHA). The CD search results show that HyleP0006 contains a GAG_lyase superfamily module (Ile⁴⁶–Pro⁷⁴⁵). By the amino acid alignment, HyleP0006 could be attributed to the PL8 family, which included the conserved catalytic residues of the PL8 family with Asn²³⁴, His²⁸⁴, and Tyr²⁹³.

2.4. Heterogenous Expression of *hyleP0006*

As depicted in Figure 5a, the strain of *E. coli* BL21(DE3)/pET-22b(+)-*hyleP0006* was successfully constructed. Subsequently, purification was successfully accomplished using affinity chromatography. In Figure 5b, a distinct band within the 75–100 kDa was observed on SDS-PAGE analysis, aligning with the anticipated size of HyleP0006 (87.88 kDa). The protein concentration measured by the Bradford method was 1.15 mg/mL, the enzyme activity was 1.1×10^6 U/mL, and the specific enzyme activity of hyaluronan lyase HyleP0006 was 9.5×10^5 U/mg.

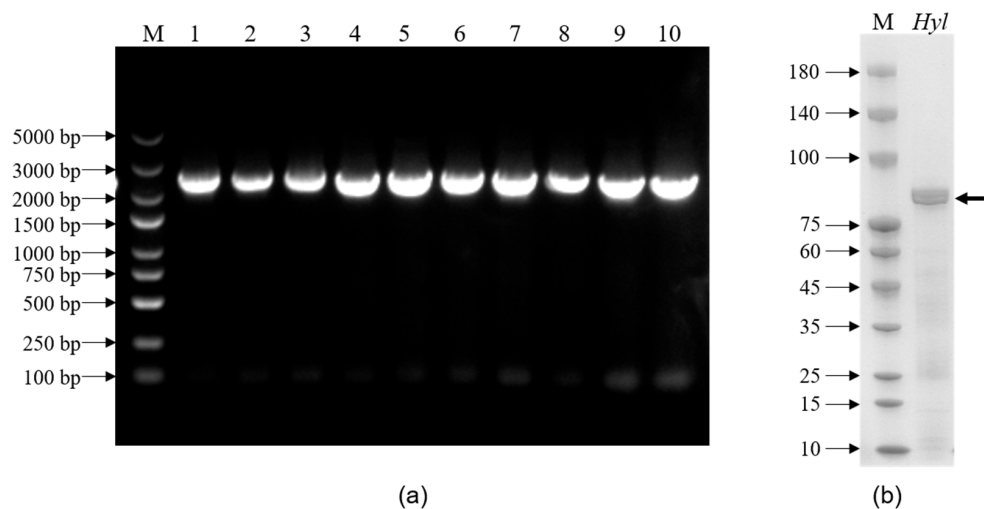


Figure 5. The expression of *hyleP0006*: (a) Colony PCR validation of the recombinant strain. Lane M: DNA marker; 1–10: PCR amplification bands of positive clones (the DNA fragment size of *hyleP0006*: 2379 bp). (b) SDS-PAGE of purified recombinant HyleP0006. Lane M, unstained protein molecular weight marker; lane Hyl, purified HyleP0006.

2.5. Biochemical Properties Characterization of HyleP0006

2.5.1. The Effects of Temperature and pH on Enzymatic Activity

The recombinant HyleP0006 exhibited maximal activity at 40 °C, as shown in Figure 6a. The stability of HyleP0006 was better at 30–35 °C, and the activity of HyleP0006 could retain about 60% when it was kept for 2 h, as shown in Figure 6b. The stability of the enzyme was poor at the temperature of 40 °C and above, and the activity rapidly decreased to less than 50% after 30 min of heat preservation.

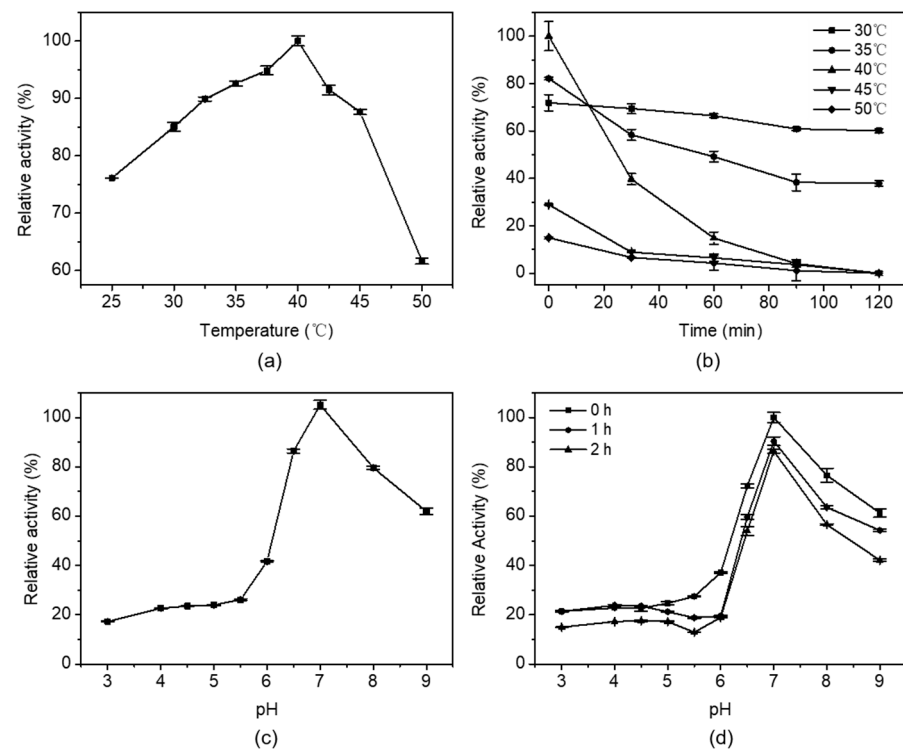


Figure 6. The effects of temperature and pH on the enzymatic activity of HyleP0006: (a) Effect of temperature. The enzymatic activity of HyleP0006 was measured at 25–50 °C. HyleP0006 had the highest specific activity at 40 °C, equivalent to 100%. (b) Thermal stability of HyleP0006. The cells were incubated at different temperatures (30–50 °C) for 2 h, and the residual activity of HyleP0006 was determined at 40 °C. The initial specific activities of HyleP0006 were all set to be 100%. (c) Effect of pH. The enzymatic activity of HyleP0006 was assessed in a 50 mM buffer solution, comprising Na₂HPO₄-Citrate buffer (pH 3.0–5.0), NaH₂PO₄-Na₂HPO₄ buffer (pH 6.0–8.0), and Glycine-NaOH buffer (pH 9.0–10.0). In NaH₂PO₄-Na₂HPO₄ buffer (pH 7.0), HyleP0006 exhibited its maximum specific activity, which was recorded as being equivalent to 100%. (d) pH stability of HyleP0006. The residual activity of HyleP0006 was assessed at a temperature of 40 °C by subjecting it to incubation in the aforementioned buffer (with pH ranging from 3.0 to 9.0) for 2 h, maintaining the incubation temperature at 30 °C. The initial specific activities of HyleP0006 were all set to be 100%. Values represent the mean of three replicates ± SD.

Figure 6c indicated that HyleP0006 was a neutral hyaluronan lyase, and the optimum pH of this enzyme was determined as pH 7.0. When the pH value was between 5.0 and 9.0, the activity was relatively stable, as shown in Figure 6d.

2.5.2. Substrate Specificity of HyleP0006

The specificity of hyaluronan lyase against different substances is also different. Table 2 showed that the HyleP0006 performed good substrate specificity and high substrate specificity for hyaluronic acid, but there was almost no degradation for chondroitin sulfate, heparin, sodium alginate, and chitosan.

Table 2. Substrate specificity of HyleP0006.

Polysaccharide Species	Relative Enzyme Activity (%)
Hyaluronic acid	100.00 ± 0.71
Chondroitin sulfate	6.33 ± 1.57
Heparin	0.88 ± 0.15
Sodium alginate	0.43 ± 0.21
Chitosan	ND

Note: ND indicates that no enzyme activity is detected. Values represent the mean of three replicates ± SD.

2.5.3. Effects of Metal Ions on HyleP0006

As shown in Table 3, when the concentration of metal ions was 1 mmol/L, Ca^{2+} can promote the activity of HyleP0006, while Al^{3+} , Cu^{2+} , Zn^{2+} , and Fe^{3+} could significantly inhibit the activity of HyleP0006. When the concentration of metal ions was increased to 10 mmol/L, both Mg^{2+} and Ca^{2+} could promote the activity of HyleP0006. With the increase in the concentration of the two metal ions, the promoting effect was more obvious, while the rest of the metal ions showed an inhibitory trend on the activity of HyleP0006.

Table 3. Effects of metal ions on HyleP0006.

Metal Ions	Relative Enzyme Activity (%)		Metal Ions	Relative Enzyme Activity (%)	
	1 mmol/L	10 mmol/L		1 mmol/L	10 mmol/L
Control	100.00 ± 2.51	100.00 ± 6.50	Ba^{2+}	92.06 ± 7.04	71.16 ± 2.54
Ca^{2+}	117.52 ± 1.80	143.43 ± 4.11	Zn^{2+}	48.42 ± 0.26	12.48 ± 2.38
Mg^{2+}	94.54 ± 3.15	152.22 ± 7.40	K^{+}	97.36 ± 2.57	74.96 ± 1.82
Li^{+}	105.52 ± 0.77	65.93 ± 2.54	Al^{3+}	7.39 ± 1.80	9.86 ± 7.40
Cu^{2+}	38.93 ± 0.58	ND	Fe^{3+}	75.96 ± 1.67	ND

Note: ND indicates that no enzyme activity is detected. Values represent the mean of three replicates ± SD.

2.5.4. Kinetic Constants of HyleP0006

Figure 7a shows the degradation of substrates at various concentrations by the HyleP0006 at 40 °C, pH 7.0. The highest concentration of HA, which was 0.16 mg/mL, was chosen to determine kinetic parameters. The affinity of HyleP0006 for HA was studied by measuring the kinetic parameters of HA at different concentrations (0.01–0.16 mg/mL). Kinetic parameters were calculated using a Lineweaver–Burk plot, as shown in Figure 7b. The maximum reaction rate of HyleP0006 was $V_{\text{max}} = 1.075 A_{232} / \text{min}$, and Michaelstrom constant $K_m = 1.636 \text{ mg/mL}$.

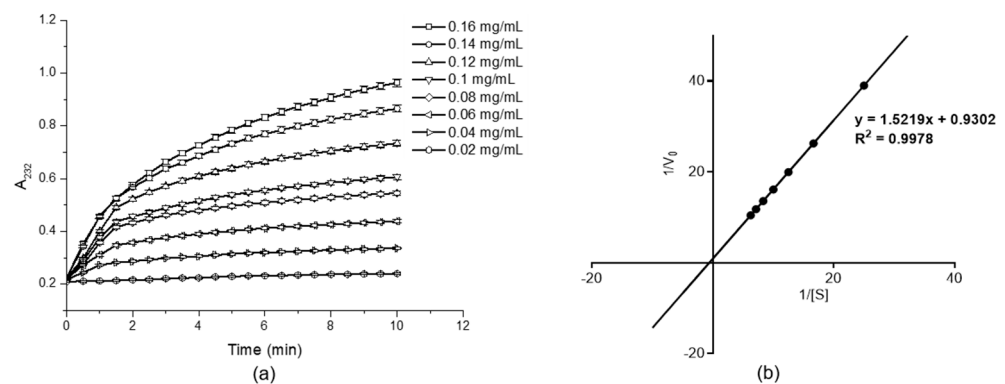


Figure 7. Enzymatic kinetic study of HyleP0006: (a) HyleP0006 degradation process of different concentrations of substrate figure. Values represent the mean of three replicates ± SD. (b) Lineweaver–Burk double reciprocal plot of HyleP0006.

2.6. Analysis of Final Degradation Product

To investigate the final degradation product of HyleP0006, hyaluronic acid with a molecular weight of 1.3×10^7 Da was subjected to enzymatic degradation. After being degraded for 1 h, the results of HPLC analysis revealed the presence of unsaturated disaccharides (HA2), hyaluronan tetrasaccharide (HA4), hyaluronan hexose (HA6), hyaluronan octadose (HA8), and hyaluronan deca-saccharide (HA10), as shown in Figure 8a. For a total degradation of hyaluronic acid for 10 h, it showed that the end product of the enzyme was HA2. To accurately determine the precise molecular weight of the end product, we employed negative ion ESI-MS. The dominant peak observed in the mass spectrum exhibited a m/z value of 378, which corresponds to the molecular weight of the unsaturated disaccharide [18], as depicted in Figure 8b. Thus, it could be concluded that HyleP0006 eventually degrades HA to unsaturated disaccharides.

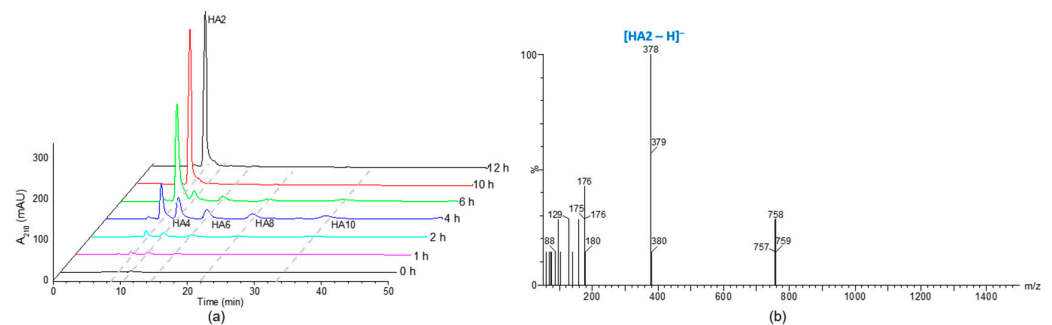


Figure 8. The analysis of HA digested by HyleP0006: (a) The final product of HA digested with HyleP0006 at 40 °C was analyzed by HPLC using a YMC-Pack Polyamine II column. (b) Analysis of the end product resulting from the digestion of HA with HyleP0006 using electrospray ionization mass spectrometry (ESI-MS).

2.7. Exploration of the Degradation Behavior of HyleP0006

To further explore the degradation behavior of enzymes, degradation experiments of purified HA4 (Figure S1) and HA10 (Figure S2) with HyleP0006 were investigated. Figure 9a shows that HA2 was generated from HA4 at 0.1 h, and no other product was generated. HA4 could be utterly degraded to HA2 at 6 h. These results indicated that the minimum degradation substrate of HyleP0006 was HA4, and the final degradation product was HA2 (Figure 9b).

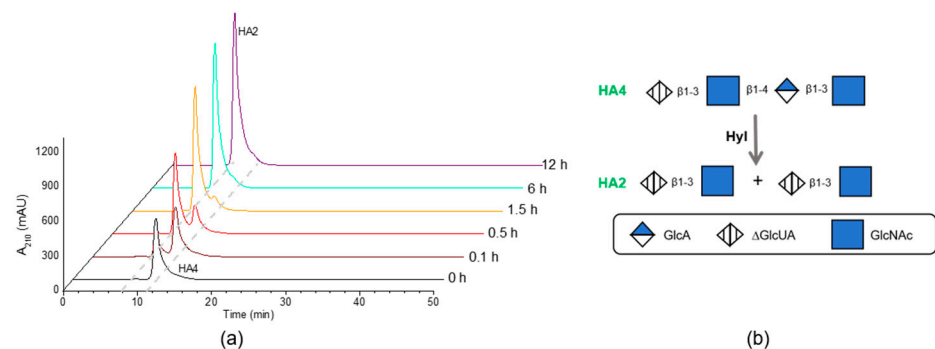


Figure 9. The analysis of HA4 degraded products by HyleP0006: (a) The product of HA4 degraded with HyleP0006 at 40 °C was analyzed by HPLC. (b) Scheme diagram of the cleavage of oligosaccharide HA4 substrates by HyleP0006.

As illustrated in Figure 10a, during the degradation process of HA10, the formation of HA2, HA4, HA6, and HA8 could be seen in HPLC profiles at 0.1 h. In detail, at 0.1 h, the concentration of HA2 was 0.0386 mmol/L, while the concentrations of HA4, HA6, and HA8 were 0.0177 mmol/L, 0.0195 mmol/L, and 0.0112 mmol/L, respectively, as showed in

Figure 10b. Moreover, during the subsequent degradation process, the concentration of HA4, HA6, and HA8 only increased slowly during the initial 1.5 h degradation period. In contrast, the concentration of HA2 increased steadily with the increase in degradation time. At the end of the degradation, HA10 was eventually degraded to HA2 at 12 h.

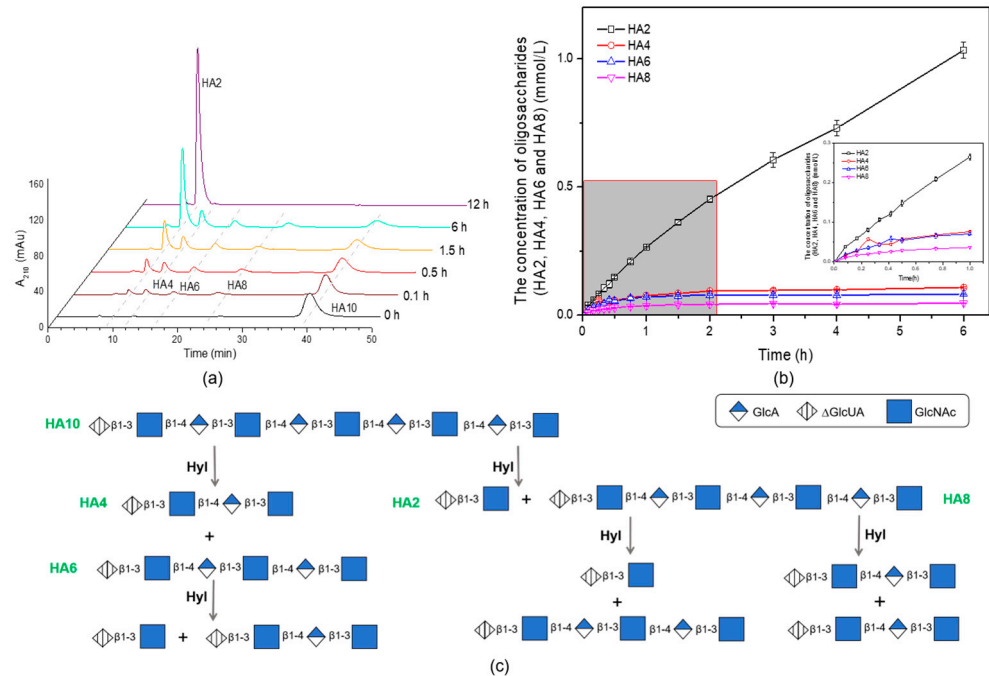


Figure 10. The analysis of HA10 degraded products by HylEP0006: (a) The product of HA10 degraded with HylEP0006 at 40 °C was analyzed by HPLC using a YMC-Pack Polyamine II column. (b) The oligosaccharide content of each product component during the initial 6 h degradation period of HA10 at 40 °C was analyzed by HPLC. Values represent the mean of three replicates \pm SD. (c) Scheme diagram of the cleavage of oligosaccharide HA10 substrates by HylEP0006.

3. Discussion

HA can be found in numerous functional marine resources, such as discarded fish eyes, loach mucus, stingray liver, and so on. For HA degradation, enzymatic processing employing hyaluronidase is highly efficient and specific, and it can be used as a potential process. Compared with animal-derived enzymes, microbial-derived enzymes have the characteristics of high yield, strong activity, diverse properties, and easy heterologous recombinant expression, which are the main research objects of industrial enzymes. In this study, a strain of *E. asburiae* CGJ001 with high hyaluronic acid degradation ability was screened from industrial wastewater. Reinforced by integrating whole-genome sequencing, we successfully acquired the comprehensive amino acid sequence and the gene encoding the hyaluronate lyase of HylEP0006. Based on bioinformatics analysis, a hyaluronic acid degradation system of PUL_{HA} in *E. asburiae* CGJ001 was identified. This PUL_{HA} was very similar to those PULs of HA in *V. alginolyticus* [18] and *Fusobacteria* [19]. In its genome, *E. asburiae* CGJ001 possesses TBDT proteins, which are the *Proteobacteria* equivalent of the SusC/SusD pair [20]. Combining genomic investigations with biochemical analysis enhanced our comprehension of PULs' role in microbial communities.

In this study, we conducted heterologous expression, purification, and characterization of hyaluronan lyase in PUL_{HA}. The strain of *E. coli* BL21(DE3)/pET-22b(+)-hylEP0006 was successfully constructed, and HylEP006 exhibited optimal degradation, showing a high activity of 9.5×10^5 U/mg. The activity of HylEP006 is higher compared to that of mammalian hyaluronidase, including *Homo sapiens*, *Bos grunniens*, and *Lachesis mutar hombeata*, as shown in Table 4. The enzyme can rapidly degrade HA and obtain HA oligosaccharides with concentrated molecular weight. The enzymatic activity of HylEP0006

was optimal at 40 °C and pH 7.0. The activity of HyleP0006 showed the same optimum temperature as that of *Bacillus* sp. CQMU-D, *Paenibacillus aquistagni* SH-7-A, *Yersinia* sp. 298, and *Escherichia* sp. A9, as shown in Table 4. Most bacterial hyaluronan lyases play their most important role in the neutral and acidic range. HyleP0006 exhibits stability at pH 6.0–9.0 and 30–35 °C, comparable to the human environment. This suggests that the HyleP0006 has great potential applications in the medical industry. Moreover, HyleP0006 is stable in a wider pH range, which is beneficial to the storage of enzyme preparations. When the concentration of metal ions increased from 1 to 10 mmol/L, Mg²⁺ and Ca²⁺ promoted the enzymatic activity of HyleP0006, while Al³⁺, Zn²⁺, and Fe³⁺ significantly inhibited the activity. Similar to *Brevibacterium halotolerans* DC1, Ca²⁺ and Mg²⁺ promote hyaluronan lyase activity, whereas Zn²⁺ inhibits hyaluronan lyase activity. HA lyases from different sources has different substrate specificities, as shown in Table 4. HyleP0006 possesses high specificity for HA and almost no ability to degrade chondroitin sulfate and heparin. Due to its specific ability to degrade HA, HyleP0006 holds great potential in extracting and utilizing marine HA resources.

Table 4. The properties of hyaluronidases from different species.

Source	Molecular Mass	Substrate Spectrum	Optimal Temperature (°C)	Optimal pH	pH Stability	Assay Method	Specific Activity (U/mg)
<i>E. asburiae</i> CGJ001 (This study)	87.88 kDa	HA	40	7	6–9	Reducing sugar method (DNS termination)	9.50 × 10 ⁵
<i>Bacillus</i> sp. A50 [21]	123 kDa	HA, CS	44	6.5	5–6	Turbidimetric method	1.02 × 10 ⁶
<i>Bacillus niacin</i> JAM F8 [16]	120 kDa	HA, CS	45	6	6–11	Ultraviolet method	136.7
<i>Brevibacterium halotolerans</i> DC1 [22]	41 kDa	HA, CS, DS, dermatan	37	7	5–9	Turbidimetric method	26.37
<i>Arthrobacter globiformis</i> A152 [23]	73.7 kDa	HA, CS	42	6	5–7	Ultraviolet method	297.2
<i>Streptococcus pyogenes</i> bacteriophage H4489A [24]	40 kDa	HA	37	5.5	4–7	Elson–Morgan-like method	9.62
<i>Paenibacillus aquistagni</i> SH-7-A [25]	110 kDa	HA	40	6	5–7	Ultraviolet method	1.18 × 10 ⁴
<i>Bacillus</i> sp. CQMU-D [26]	126.2 kDa	HA, CS	40	7	7–10	Ultraviolet method	-
<i>Thermasporomyces copostie</i> DSM22891 [27]	90 kDa	HA	70	5.93	6.1–10.9	Ultraviolet method	10.91
<i>Yersinia</i> sp. 298 [28]	115.4 kDa	HA, CS	40	7.5	6.0–11.0	Ultraviolet method	11.19
<i>Escherichia</i> sp. A99 [29]	86.7 kDa	HA, CS	40	6	5.5–6.6	Ultraviolet method	376.32
<i>Homo sapiens</i> [30]	48.3 kDa	HA	-	3.5–4.0	-	Elson–Morgan-like method	6.8
<i>Bos grunniens</i> [31]	55 kDa	HA, CS and DS	37	3.8	-	Elson–Morgan-like method	20.4
<i>Lachesis muta rhombeata</i> [32]	60 kDa	-	37	6	-	Turbidimetric method	-

Note: The enzyme activity definition of 1 U determined with various methods: Turbidimetric method—the amount of enzyme required to make 1 µmol hyaluronic acid turbidity vanished per minute; DNS termination—the amount of enzyme required to degrade hyaluronic acid to form 1 µg reducing sugar per hour; Elson–Morgan-like method—the amount of enzyme required to releases 1 µmol of the unsaturated oligomers produced per minute; Ultraviolet method—the amount of enzyme required to degrade hyaluronic acid to form 1 µmol of unsaturated double bonds per minute.

HyleP0006 was used to degrade the hyaluronan polysaccharide, which was completely degraded at 12 h of degradation, and the product was a singly unsaturated hyaluronan disaccharide. Like most hyaluronan lyases, the final degradation product is an unsaturated

hyaluronan disaccharide. The degradation mode of HyleP0006 was further explored. The purified enzyme efficiently degraded a singular substrate (HA4), resulting in complete degradation to HA2 within 6 h, as shown in Figure 9a. This indicated that the minimal binding substrate of the enzyme was unsaturated hyaluronan tetrasaccharide, and a schematic diagram of the degradation is shown in Figure 9b. Degradation of the single substrate HA10 with purified enzymes resulted in the formation of HA2. Similarly, after 12 h, all HA10 was degraded to HA2 (Figure 10a). As illustrated in Figure 10b, HA2, HA4, HA6, and HA8 were all generated at 0.1 h, indicating that HA2 was not the only product generated by HyleP0006. The concentrations of HA4 and HA6 fluctuated at 0.3 h and 0.5 h, respectively, which could be attributed to the fact that the amounts of HA4 and HA6 being degraded by HyleP0006 at that time were higher than those produced. In addition, the concentrations of HA4, HA6, and HA8 increased slowly during the initial 1.5 h degradation period, while the concentration of HA2 increased steadily with the increase in degradation time. Therefore, it indicated that HyleP0006 exhibited a higher propensity for generating unsaturated hyaluronic acid disaccharides during the degradation of HA. The mechanism diagram of HyleP0006 in the degradation of HA is shown in Figure 10c. HyleP0006 not only degrades HA in a short time but also obtains relatively pure unsaturated HA2. The excavation of HyleP0006 supplements the resources of hyaluronate lyase. It could be beneficial to further studies of activity assessments of HA oligosaccharides.

4. Materials and Methods

4.1. Materials

HA (1.3×10^7 Da) was obtained from Focus Freda (Jinan, China). Restriction endonucleases were purchased from Takara, and DNA polymerases, DNA purification kit, gel extraction kit, and plasmid miniprep kit were obtained from Vazyme (Nanjing, China). All other reagents were purchased from commercial sources.

4.2. Methods

4.2.1. Isolation of Hyaluronate Lyase-Producing Bacteria

Samples were obtained from waste water near factories producing HA, and 1 mL of the supernatant was added to 9 mL of normal saline and diluted to five concentration gradients of 10^{-4} , 10^{-5} , 10^{-6} , 10^{-7} , and 10^{-8} , respectively. The diluted bacterial suspension was spread on the primary screening medium. Two parallel cultures were made for each concentration and incubated at 30 °C for 5 days. Well-grown single colonies were picked out, through liquid medium cultivation, coated in solid medium, and then picked out in seed liquid medium, cultured for 24 h at 30 °C, 220 rpm. The cells were collected by centrifugation, resuspended in NaH_2PO_4 - Na_2HPO_4 buffer (pH 7.0), sonicated and centrifuged to obtain the crude enzyme solution. The enzyme activity was determined, and the strain with high enzyme activity was screened out.

4.2.2. Enzyme Activity Assays

The activity of hyaluronate lyase was measured as described above. Briefly, 0.9 mL, 2 g/L HA (dissolved in 50 mM, pH 7.0 NaH_2PO_4 - Na_2HPO_4 buffer) was reacted with 0.1 mL of the enzyme solution. The released reducing sugar was determined by the 3, 5-dinitrosalicylic acid (DNS) assay, and the absorbance at 540 nm was measured. One unit of the activity of hyaluronate lyase was defined as the amount of enzyme required to release 1.0 μg of reducing sugar, equivalent to glucose, per hour after hydrolysis of HA at the optimal reaction temperature [33].

4.2.3. Identification of Strain *Enterobacter* sp. CGJ001

The forward primer 27f: 5'-AGTTTGATCCTGGCTCAG-3' and the reverse primer 1492r: 5'-GCTTACCTTGTACGACTT-3' were used for 16S rDNA gene amplification of strains. The program used for strain gene amplification consists of pre-denaturation at 95 °C for 10 min, denaturation at 95 °C for 30 s, annealing at 55 °C for 30 s, extension at

72 °C for 90 s, a total of 34 cycles, extension at 72 °C for 15 min, and insulation at 4 °C. By blast in the NCBI database for sequence alignment (<http://blast.ncbi.nlm.nih.gov/Blast.cgi>, accessed on 5 April 2022), the phylogenetic tree was generated by MEGA X using the neighbor-joining method [34].

4.2.4. Genome Sequencing and Sequence Analysis

Strain *E. asburiae* CGJ001 was fermented in a culture medium for 24 h at a temperature of 30 °C. Following this, the cells were collected by centrifugation at 12,000 rpm at 4 °C for 10 min. Subsequently, the cell collection was sent to Suzhou Golden Extreme Intelligence Technology Co., Ltd. (Suzhou, China), to extract genomic DNA. The whole genome of the strain was sequenced. Based on the assembly results, the genome components, such as functional genes, non-coding RNA, and repetitive sequences, were analyzed. For the predicted genes, the sequence similarity was compared with the relevant database (KEGG, COG, and GO) to obtain the gene function [35].

4.2.5. Sequence Analysis of HyleP0006

The NCBI PDB and Nr databases were searched for similarity using the online Blastp algorithm. Protein modules and domains were analyzed using conserved domain (CD) search technology. The presence and pattern of signal peptides were identified using the SignalP 5.0 server (<http://www.cbs.dtu.dk/services/SignalP>, accessed on 5 May 2023). The ProtParam tool on the ExPASy server (<http://www.expasy.org>, accessed on 15 May 2023) was utilized to predict the physicochemical characteristics of proteins, including Mw and pI.

4.2.6. Molecular Cloning, Protein Expression, and Purification

Using the primers of *hyleP0006*-F (5'-aattaattcggatccgaattcATGGATCGGATCGATAT AAGCAC-3') and primer *hyleP0006*-R (5'-ctcgagtgcggccgcaagcttTTATTCATTGGCAGGTA GCTGATAG-3'), *hyleP0006* was cloned to its full-length gene. The gene fragment was linked between *Eco*R I and *Hind* III sites of *pET*-22b(+). The recombinant plasmid *pET*-22b(+)-*hyleP0006* was transformed into *E. coli* BL21(DE3) cells. The *pET*-22b(+)-*hyleP0006* was sequenced at Tianlin Biological Co., Ltd., Shanghai, China. Recombinant bacteria cultivation in Luria–Bertani (LB) medium 37 °C, when OD₆₀₀ reached 0.4, 0.02 mM isopropyl β-D-thiogalactoside (IPTG) was added in, and *E. coli* BL21(DE3)/*pET*-22b(+)-*hyleP0006* was induced at 20 °C for 24 h. The cells were collected by centrifugation, resuspended in NaH₂PO₄-Na₂HPO₄ buffer (pH 7.0), sonicated and centrifuged to obtain the crude enzyme solution. The recombinant hyaluronate lyase containing C-terminal (His)₆ tags was purified using Histrap column (Beyotime Biotechnology, Shanghai, China) chromatography from the supernatant solution. The enzyme was collected for characterization, and its purity was verified by sodium dodecyl sulfate-polyacrylamide gel electrophoresis (SDS-PAGE). Protein concentration was determined using the BCA Protein Assay kit (Beyotime Biotechnology, Shanghai, China).

4.2.7. Characterization of HyleP0006

HyleP0006 and HA were incubated at different temperatures (25, 30, 32.5, 35, 37.5, 40, 42.5, 45, and 50 °C) to determine the optimum temperature of HyleP0006. The enzyme was kept at different temperatures (30, 35, 40, 45, and 50 °C) for 2 h, and the enzyme activity was measured every 30 min to investigate the thermal stability of HyleP0006. HyleP0006 and HA were incubated at different pH, including Na₂HPO₄-Citrate buffer (pH 3.0–5.0), NaH₂PO₄-Na₂HPO₄ buffer (pH 6.0–8.0), and Glycine-NaOH buffer (pH 9.0–10.0), to determine the optimal reaction pH of HyleP0006. The enzyme was incubated in buffer with different pH, including Na₂HPO₄-Citrate buffer (pH 3.0–5.0), NaH₂PO₄-Na₂HPO₄ buffer (pH 6.0–8.0), and Glycine-NaOH buffer (pH 9.0–10.0), for 2 h, and the enzyme activity was measured every 1 h to explore the stability of HyleP0006 in different pH buffers. The substrate of the enzyme was changed, and HyleP0006 was used to degrade 2 g/L HA,

chondroitin sulfate, heparin, sodium alginate, and chitosan, respectively. The activity of HyleP0006 for degrading HA was used as a control of 100%; the relative enzyme activities of the experimental groups were calculated. To explore the effect of metal ions on hyaluronidase, various metal ion solutions were prepared at the concentrations of 1 mM and 10 mM, respectively (Al^{3+} , Mg^{2+} , Cu^{2+} , Zn^{2+} , Fe^{3+} , Ba^{2+} , Li^+ , K^+ , Ca^{2+}). The enzyme activity was determined after being incubated at 30 °C for 30 min in different ion solutions, with the activity in NaH_2PO_4 - Na_2HPO_4 buffer as the control of 100%. The relative enzyme activities of the experimental groups were calculated.

4.2.8. Analysis of Kinetic Parameters

Different concentrations of HA solutions (0.02, 0.04, 0.06, 0.08, 0.10, 0.12, 0.14, and 0.16 g/L) were prepared as the reaction substrate, and the activity of HyleP0006 was determined under the optimal conditions. The enzymatic kinetic parameters of HyleP0006 were calculated using nonlinear analysis with GraphPad Prism 8.0 (GraphPad Software, Inc., San Diego, CA, USA).

4.2.9. Analysis of Degradation Products of HyleP0006

HPLC was employed for product analysis. The detailed method included: YMC-Pack Polyamine chromatographic column II (250 mm × 4.6 mm, 5 μm), mobile phase: 0.1 mol/L NaH_2PO_4 solution: Acetonitrile ($v/v = 90:10$), UV detection at 210 nm, column temperature at 30 °C, flow rate at 0.5 mL/min, and loading volume at 5 μL. The negative ion electrospray ionization mass spectrometry (ESI-MS, MALDI SYNAPT MS, Hilo, HI, USA) was utilized to determine the Mw of the end product accurately. The mass spectrum collection range: 50–2000 m/z . The ESI-MS analysis was performed under the following conditions: Capillary: 3.0 kV, Cone: 20/50 V, Source Block Temp: 100 °C, Desolvation Temp: 400 °C, Desolvation Gas Flow: 700 L/h, Cone Gas Flow: 50 L/h, Collision Energy: 6 eV, Detector: 1800 V [36].

4.2.10. The Degradation Behavior Exploration of HyleP0006

The degradation behavior of HyleP0006 towards HA was studied. For the enzymatic reaction, the ratio of enzyme and substrate was unified as 10 U/mg. A 20 mL solution of HA (0.1%, w/v) was digested with purified HyleP0006 for 12 h at 40 °C. The samples were taken at incubation times of 1, 2, 4, 6, 10 and 12 h. For further exploration of the reaction detail, HA4 and HA10 were separated and employed as the substrates. The samples were taken at 0.1, 0.3, 0.5, 1, 1.5, 6, and 12 h. All of the samples were subjected to thermal inactivation at 100 °C for 10 min, followed by 12,000 rpm for 10 min. Subsequently, filtration was performed using a cellulose acetate membrane (0.22 μm) for HPLC analysis.

4.2.11. Statistical Analysis

All experiments were conducted in triplicate, and the results are presented in tables and graphs as mean values accompanied by their corresponding standard deviations.

5. Conclusions

In this study, a high hyaluronan lyase-producing strain, *E. asburiae* CGJ001, was screened from wastewater. In conjunction with the analysis of whole-genome sequencing, it was discovered that *E. asburiae* CGJ001 harbors a cluster of genes related to the degradation, transportation, and metabolism of HA. The strain of *E. coli* BL21(DE3)/*pET-22b(+)-hyleP0006* was successfully constructed, and HyleP0006 exhibited optimal degradation at 40 °C and pH 7.0, showing a high activity of 9.50×10^5 U/mg. The minimal binding substrate of HyleP0006 was an unsaturated tetrasaccharide of hyaluronic acid, and HyleP0006 efficiently prepared unsaturated disaccharides. This research aims to enhance the utilization potentiality of hyaluronan lyase across various industries, including medicine, cosmetics, and food sectors. In addition, the extraction and utilization of marine hyaluronic acid resources are promoted through microbial-derived enzymes.

Supplementary Materials: The following supporting information can be downloaded at: <https://www.mdpi.com/article/10.3390/md22090399/s1>, Figure S1: Analysis of HA4: (a) Structure of HA4; (b) HA4 was analyzed by HPLC using a YMC-Pack Polyamine II column. (c) Analysis of HA4 using electrospray ionization mass spectrometry (ESI-MS); Figure S2: Analysis of HA10: (a) Structure of HA10; (b) HA10 was analyzed by HPLC using a YMC-Pack Polyamine II column. (c) Analysis of HA10 using ESI-MS.

Author Contributions: Conceptualization, L.Z. and J.S.; methodology, J.J.; software, W.L.; validation, L.W.; formal analysis, Z.Y.; investigation, H.L.; resources, C.K. and L.L.; data curation, J.G.; writing—original draft preparation, L.Z.; writing—review and editing, H.L.; visualization, J.G.; supervision, Z.X.; project administration, J.S.; funding acquisition, J.S. All authors have read and agreed to the published version of the manuscript.

Funding: This work was financially supported by the National Key Research and Development Program of China (No. 2021YFC2102000), the National Natural Science Foundation of China (No. 22278181), and Taishan Industry Leading Talent of Shandong Province (No. tscx202211017).

Data Availability Statement: All data analyzed during this study are included in this published article.

Conflicts of Interest: Chuanli Kang and Lei Liu are employed by Shandong Focusfreda Biotech Co., Ltd. All other authors declare that there are no potential conflicts of interest. Shandong Focusfreda Biotech Co., Ltd. has no known competing financial interests or personal relationships that could have appeared to influence the work reported in this paper.

References

1. Zhang, Y.-S.; Gong, J.-S.; Yao, Z.-Y.; Jiang, J.-Y.; Su, C.; Li, H.; Kang, C.-L.; Liu, L.; Xu, Z.-H.; Shi, J.-S. Insights into the source, mechanism and biotechnological applications of hyaluronidases. *Biotechnol. Adv.* **2022**, *60*, 108018. [[CrossRef](#)]
2. Kogan, G.; Soltes, L.; Stern, R.; Gemeiner, P. Hyaluronic acid: A natural biopolymer with a broad range of biomedical and industrial applications. *Biotechnol. Lett.* **2007**, *29*, 17–25. [[CrossRef](#)] [[PubMed](#)]
3. Murado, M.A.; Montemayor, M.I.; Cabo, M.L.; Vázquez, J.A.; González, M.P. Optimization of extraction and purification process of hyaluronic acid from fish eyeball. *Food Bioprod. Process.* **2012**, *90*, 491–498. [[CrossRef](#)]
4. Stern, R.; Asari, A.A.; Sugahara, K.N. Hyaluronan fragments: An information-rich system. *Eur. J. Cell Biol.* **2006**, *85*, 699–715. [[CrossRef](#)] [[PubMed](#)]
5. Karbownik, M.S.; Nowak, J.Z. Hyaluronan: Towards novel anti-cancer therapeutics. *Pharmacol. Rep.* **2013**, *65*, 1056–1074. [[CrossRef](#)] [[PubMed](#)]
6. Toole, B.P.; Ghatak, S.; Misra, S. Hyaluronan oligosaccharides as a potential anticancer therapeutic. *Curr. Pharm. Biotechnol.* **2008**, *9*, 249–252. [[CrossRef](#)]
7. Aya, K.L.; Stern, R. Hyaluronan in wound healing: Rediscovering a major player. *Wound Repair. Regen.* **2014**, *22*, 579–593. [[CrossRef](#)] [[PubMed](#)]
8. Termeer, C.; Benedix, F.; Sleeman, J.; Fieber, C.; Voith, U.; Ahrens, T.; Miyake, K.; Freudenberg, M.; Galanos, C.; Simon, J.C. Oligosaccharides of Hyaluronan activate dendritic cells via toll-like receptor 4. *J. Exp. Med.* **2002**, *195*, 99–111. [[CrossRef](#)]
9. Du, W.; Yang, X.; He, S.; Wang, J.; Guo, Y.; Kou, B.; Jiang, Y.; Bian, P.; Li, B.; Yin, L. Novel hyaluronic acid oligosaccharide-loaded and CD44v6-targeting oxaliplatin nanoparticles for the treatment of colorectal cancer. *Drug Deliv.* **2021**, *28*, 920–929. [[CrossRef](#)]
10. Boltje, T.J.; Buskas, T.; Boons, G.J. Opportunities and challenges in synthetic oligosaccharide and glycoconjugate research. *Nat. Chem.* **2009**, *1*, 611–622. [[CrossRef](#)]
11. Yuan, P.; Lv, M.; Jin, P.; Wang, M.; Du, G.; Chen, J.; Kang, Z. Enzymatic production of specifically distributed hyaluronan oligosaccharides. *Carbohydr. Polym.* **2015**, *129*, 194–200. [[CrossRef](#)] [[PubMed](#)]
12. Jin, P.; Kang, Z.; Zhang, N.; Du, G.; Chen, J. High-yield novel leech hyaluronidase to expedite the preparation of specific hyaluronan oligomers. *Sci. Rep.* **2014**, *4*, 4471. [[CrossRef](#)]
13. Huang, L.; Huang, X. Highly efficient syntheses of hyaluronic acid oligosaccharides. *Chemistry* **2007**, *13*, 529–540. [[CrossRef](#)]
14. Weijers, C.A.; Franssen, M.C.; Visser, G.M. Glycosyltransferase-catalyzed synthesis of bioactive oligosaccharides. *Biotechnol. Adv.* **2008**, *26*, 436–456. [[CrossRef](#)] [[PubMed](#)]
15. Kurata, A.; Nishimura, M.; Kishimoto, N.; Kobayashi, T. Draft Genome Sequence of a Deep-Sea Bacterium, *Bacillus niacini* Strain JAM F8, Involved in the Degradation of Glycosaminoglycans. *Genome Announc.* **2014**, *2*, 10–1128. [[CrossRef](#)]
16. Kurata, A.; Matsumoto, M.; Kobayashi, T.; Deguchi, S.; Kishimoto, N. Hyaluronate Lyase of a Deep-Sea *Bacillus niacini*. *Mar. Biotechnol.* **2015**, *17*, 277–284. [[CrossRef](#)]
17. Mori, T.; Masuzawa, N.; Kondo, K.; Nakanishi, Y.; Chida, S.; Uehara, D.; Katahira, M.; Takeda, M. A heterodimeric hyaluronate lyase secreted by the activated sludge bacterium *Haliscomenobacter hydrossis*. *Biosci. Biotechnol. Biochem.* **2023**, *87*, 256–266. [[CrossRef](#)]

18. Wang, X.; Wei, Z.; Wu, H.; Li, Y.; Han, F.; Yu, W. Characterization of a Hyaluronic Acid Utilization Locus and Identification of Two Hyaluronate Lyases in a Marine Bacterium *Vibrio alginolyticus* LWW-9. *Front. Microbiol.* **2021**, *12*, 696096. [[CrossRef](#)]
19. Kawai, K.; Kamochi, R.; Oiki, S.; Murata, K.; Hashimoto, W. Probiotics in human gut microbiota can degrade host glycosaminoglycans. *Sci. Rep.* **2018**, *8*, 10674. [[CrossRef](#)] [[PubMed](#)]
20. Blanvillain, S.; Meyer, D.; Boulanger, A.; Lautier, M.; Guynet, C.; Denancé, N.; Vasse, J.; Lauber, E.; Arlat, M. Plant Carbohydrate Scavenging through TonB-Dependent Receptors: A Feature Shared by *Phytopathogenic* and *Aquatic bacteria*. *PLoS ONE* **2007**, *2*, e224. [[CrossRef](#)]
21. Sanchez-Ruiz, J.M.; Guo, X.; Shi, Y.; Sheng, J.; Wang, F. A Novel Hyaluronidase Produced by *Bacillus* sp. A50. *PLoS ONE* **2014**, *9*, e94156.
22. Patil, S.P.; Shirsath, L.P.; Chaudhari, B.L. A halotolerant hyaluronidase from newly isolated *Brevibacterium halotolerans* DC1: Purification and characterization. *Int. J. Biol. Macromol.* **2021**, *166*, 839–850. [[CrossRef](#)] [[PubMed](#)]
23. Zhu, C.; Zhang, J.; Li, L.; Zhang, J.; Jiang, Y.; Shen, Z.; Guan, H.; Jiang, X. Purification and Characterization of Hyaluronate Lyase from *Arthrobacter globiformis* A152. *Appl. Biochem. Biotechnol.* **2016**, *182*, 216–228. [[CrossRef](#)]
24. El-Safory, N.S.; Lee, G.-C.; Lee, C.-K. Characterization of hyaluronate lyase from *Streptococcus pyogenes* bacteriophage H4489A. *Carbohydr. Polym.* **2011**, *84*, 1182–1191. [[CrossRef](#)]
25. Li, H.; Zhang, X.; Zou, W.; Wang, T.; He, W.; Wang, L. Hyaluronidase from *Paenibacillus aquistagni* SH-7-A: Identification and characterization. *Int. Biodeterior. Biodegrad.* **2024**, *187*, 105708. [[CrossRef](#)]
26. Wang, Z.; Sun, J.; Li, Y.; Song, G.; Su, H.; Yu, W.; Gong, Q. Cloning, expression, and characterization of a glycosaminoglycan lyase from *Vibrio* sp. H240. *Enzym. Microb. Technol.* **2022**, *154*, 109952. [[CrossRef](#)] [[PubMed](#)]
27. Li, Y.; Zhang, S.; Wu, H.; Wang, X.; Yu, W.; Han, F. Biochemical characterization of a thermophilic hyaluronate lyase TcHly8C from *Thermasporomyces composti* DSM22891. *Int. J. Biol. Macromol.* **2020**, *165*, 1211–1218. [[CrossRef](#)]
28. Zhang, S.; Li, Y.; Han, F.; Yu, W. YsHyl8A, an Alkalophilic Cold-Adapted Glycosaminoglycan Lyase Cloned from *Pathogenic Yersinia* sp. 298. *Molecules* **2022**, *27*, 2897. [[CrossRef](#)]
29. Cui, X.; Fu, Z.; Wang, H.; Yu, W.; Han, F. Cloning and characterization of a hyaluronate lyase EsHyl8 from *Escherichia* sp. A99. *Protein Expr. Purif.* **2024**, *223*, 106551. [[CrossRef](#)]
30. Hofinger, E.S.A.; Spickenreither, M.; Oschmann, J.; Bernhardt, G.; Rudolph, R.; Buschauer, A. Recombinant human hyaluronidase Hyal-1: Insect cells versus *Escherichia coli* as expression system and identification of low molecular weight inhibitors. *Glycobiology* **2007**, *17*, 444–453. [[CrossRef](#)]
31. Li, R.-R.; Yu, Q.-L.; Han, L.; Rong, L.-Y.; Yang, M.-M.; An, M.-R. Isolation and enzymatic characterization of the first reported hyaluronidase from Yak (*Bos grunniens*) testis. *Korean J. Chem. Eng.* **2014**, *31*, 2027–2034. [[CrossRef](#)]
32. Wiezel, G.A.; dos Santos, P.K.; Cordeiro, F.A.; Bordon, K.C.F.; Selistre-de-Araújo, H.S.; Ueberheide, B.; Arantes, E.C. Identification of hyaluronidase and phospholipase B in *Lachesis muta rhombeata* venom. *Toxicon* **2015**, *107*, 359–368. [[CrossRef](#)]
33. Jin, P.; Kang, Z.; Yuan, P.; Du, G.; Chen, J. Production of specific-molecular-weight hyaluronan by metabolically engineered *Bacillus subtilis* 168. *Metab. Eng.* **2016**, *35*, 21–30. [[CrossRef](#)] [[PubMed](#)]
34. Kumar, S.; Stecher, G.; Li, M.; Knyaz, C.; Tamura, K. MEGA X: Molecular Evolutionary Genetics Analysis across Computing Platforms. *Mol. Biol. Evol.* **2018**, *35*, 1547–1549. [[CrossRef](#)] [[PubMed](#)]
35. Nawrocki, E.P.; Burge, S.W.; Alex, B.; Jennifer, D.; Eberhardt, R.Y.; Eddy, S.R.; Floden, E.W.; Gardner, P.P.; Jones, T.A.; John, T. Rfam 12.0: Updates to the RNA families database. *Nucleic Acids Res.* **2015**, *43*, D130–D137. [[CrossRef](#)]
36. Lv, M.; Wang, M.; Cai, W.; Hao, W.; Yuan, P.; Kang, Z. Characterisation of separated end hyaluronan oligosaccharides from leech hyaluronidase and evaluation of angiogenesis. *Carbohydr. Polym.* **2016**, *142*, 309–316. [[CrossRef](#)] [[PubMed](#)]

Disclaimer/Publisher’s Note: The statements, opinions and data contained in all publications are solely those of the individual author(s) and contributor(s) and not of MDPI and/or the editor(s). MDPI and/or the editor(s) disclaim responsibility for any injury to people or property resulting from any ideas, methods, instructions or products referred to in the content.